Keynote Lecture

Proceedings of the

First International Conference on
Marine Research and Transportation (ICMRT '05)

Ischia, Italy
September 19–21, 2005

The Separation of the Flow Past a Transom Stern

Lawrence J. Doctors

School of Mechanical and Manufacturing Engineering
The University of New South Wales
Sydney, NSW 2052, Australia

Robert F. Beck

Department of Naval Architecture and Marine Engineering
University of Michigan
Ann Arbor, MI 48109-2145, USA

The Separation of the Flow Past a Transom Stern

Lawrence J. Doctors
The University of New South Wales
Sydney, NSW 2052, Australia

Robert F. Beck
University of Michigan
Ann Arbor, MI 48109-2145, USA

Summary

We describe here an extensive set of experiments on a transom-stern ship model. The geometry of the hollow in the water behind the model was measured for a large number of cases.

This data has been reanalyzed and a new regression formula for the progressive unwetting of the transom has been developed. This formula takes into account both the transom beam-to-draft ratio and the Reynolds number. There is evidence that the Reynolds number plays an important rôle in this process. A similar regression equation has been developed for the length of the transom-stern hollow.

Using these two new formulas, one can now predict the drag components with greater confidence. Hence, the drag of a high-speed vessel with a transom stern can be estimated accurately over the entire speed range.

Principal Nomenclature

B	=	Waterline beam
D	=	Vessel depth
F	=	Froude number
F_T	=	Transom-draft Froude number
F_T^*	=	Critical transom-draft Froude number
L	=	Waterline length
L^*	=	Length of transom-stern hollow
N_{fit}	=	Coefficients in regression equation
R^2	=	Correlation coefficient in regression
R_F	=	Frictional resistance
R_H	=	Hydrostatic resistance
R_{NT}	=	Transom-draft Reynolds number
R_T	=	Total resistance
R_W	=	Wave resistance
T	=	Draft
T^*	=	Dynamic draft
U	=	Speed
W	=	Displacement weight
e_{RMS}	=	RMS error in regression equation
$e_{\max}$	=	Maximum error in regression equation
f_F	=	Frictional-resistance form factor
s	=	Sinkage of vessel
t	=	Trim of vessel
x, y, z	=	Cartesian coordinates
α	=	Wave-smoothing parameter
ζ	=	Wave elevation
ζ^*	=	Wave elevation at transom
η_{dry}	=	Unwetting function
σ	=	Wave-correction factor

1 Introduction

1.1 Prediction of Resistance

Many high-speed displacement or semi-displacement marine vessels are designed with transom or cutoff sterns. The reason for choosing such an apparently unstreamlined form is subject to debate.

A commonly given explanation is that this design feature allows the straightforward installation of a waterjet propulsion system in the stern of the vessel. On the other hand, it is also possible to make the case that the resistance of a suitably shaped transom-stern vessel can be less than that of the equivalent streamlined or sharp-ended form. Theoretical parametric resistance studies undertaken by Doctors (1999b) demonstrated that an appropriate choice of the sectional area of the transom can indeed lead to this surprising outcome. It is thought that this positive result is due to the formation of the hollow in the water behind the transom, which generates a virtual extension to the length of the vessel; this creates a favorable effective Froude number based on the overall hydrodynamic length of the vessel together with the hollow.

In a series of publications, Toby (1987, 1997, and 2002) presented in-depth discussions on the desired hull form to minimize resistance. He made a similar case for the hydrodynamic advantages of a transom stern. He based his arguments on the creation of the hollow in the water and, hence, effectively increasing the wavemaking length of the vessel. He also noted the importance of the choice of the optimal size of the transom. That is, the ratio of the submerged-transom area to the maximum-section area.

A practical procedure for analyzing such high-speed and slender vessels is to employ the classic thin-ship method of Michell (1898), together with a suitable heuristic model for the transom-stern hollow. To this end, one can consult the work of Molland, Wellicome, and Couser (1994) and Couser, Wellicome, and Molland (1998). These researchers appear to be the

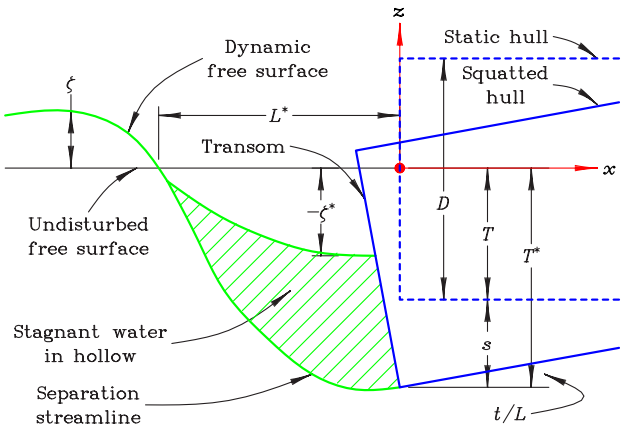

Figure 1: Definition of the Problem
(a) Geometric Parameters

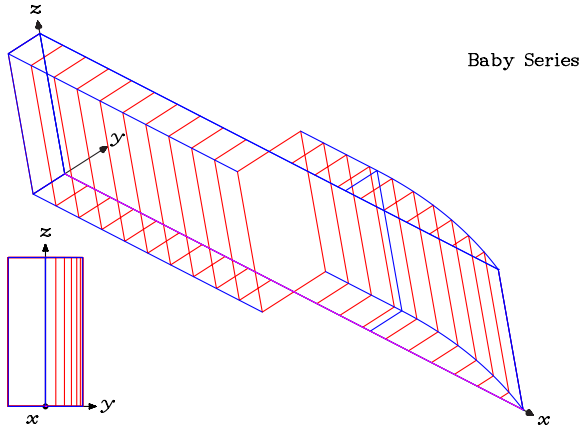

Figure 1: Definition of the Problem
(b) Parent Hull for Baby Series

first who developed this useful technique. This approach for modeling the transom hollow prescribed a hollow length that was invariant with the speed of the vessel. As a consequence, Doctors and Day (1997) improved the idea by means of their "firehose" model. This model ensured that the transom hollow constituted a truly continuous extension of the surface of the hull — rather akin to satisfying the Kutta condition. Furthermore, the length of the hollow increased with the speed of the vessel in a plausible manner.

This approach has been developed in a number of publications. In particular, the concept of applying both a wave-resistance form factor and a frictional-resistance form factor has been shown to be most effective for increasing the accuracy of the predictions of the total resistance. This effort has been reported by Doctors (1998a, 1998b, and 1999a) and Sahoo, Doctors, and Renilson (1999).

The analysis of the resistance of the vessel can be extended to the case of water of restricted width and depth. This situation pertains to a ship sailing in a canal or to the test of a ship model in a towing tank. Quite practical predictions of resistance for such cases have been reported by Doctors and Renilson (1992). This is based on the work of Sretensky (1936) and Lunde (1951), in which the necessary complications of the restricted water were detailed. Excellent correlation between theory and experiments for the resistance of a transom-stern ship model was also demonstrated by Sahoo and Doctors (2003).

A more sophisticated analysis is one in which the near field is computed. A series of papers on this technique includes the work of Doctors and Day (2000a, 2000b, 2002a, and 2002b). In this analysis, the actual pressure distribution on the surface of the hull is computed, rather than the energy radiated in the far-field behind the vessel. The advantage of the computer-time-consuming near-field approach is that the sinkage and the trim of the vessel can also be predicted, in addition to the resistance.

1.2 Transom Flow

In the work of Doctors and Day (1997), it was assumed that the water separated completely behind the transom. That is, a fully-ventilated condition was simply modeled. As a consequence, the theoretically challenging matter of a partly-ventilated transom was not considered. It is clear that the resulting predictions for the resistance in the low-speed régime will be too high.

A brief note in the work of Oving (1985) seems to be one of the earliest references to the question of the partly-ventilated transom. In that report, he provided a semi-empirical formula for estimating the drop in the water level in the essentially stagnant flow region just aft of the transom. His formula yields the critical value of the transom-draft Froude number $F_T = U/\sqrt{gT}$, as a function of the beam-to-draft ratio B/T, as follows:

$$F_T^* = \begin{cases} 4.95 - 1.2B/T & \text{for } B/T \leq 2.50 \\ 1.95 & \text{for } B/T \geq 2.50 \end{cases} \quad .(1)$$

Here, U is the speed of the vessel and g is the acceleration due to gravity.

Doctors and Day (2002b) tried a simple but effective approach for estimating the drop in level of the free surface immediately behind the transom stern. Here, it was considered that the suction behind the transom was analogous to the suction that is created behind a bluff-ended body. That is, one should be able to assume a suitable pressure coefficient that is relatively independent of the Reynolds number.

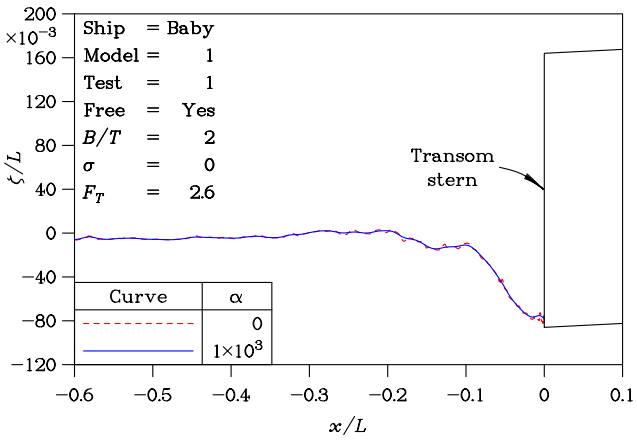

Figure 2: Numerical Smoothing of Wave Profile for Free Trim (a) $F_T = 2.6$

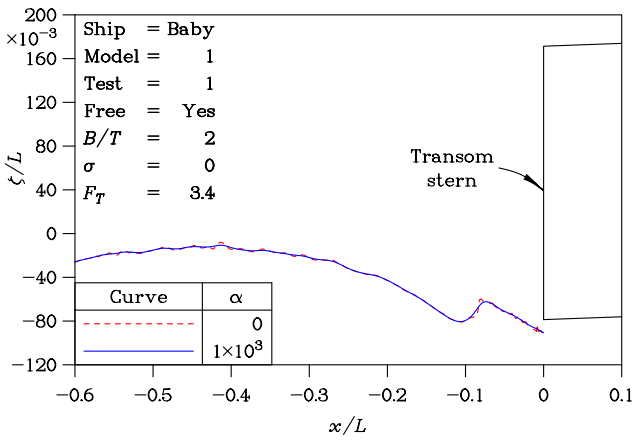

Figure 2: Numerical Smoothing of Wave Profile for Free Trim (b) $F_T = 3.4$

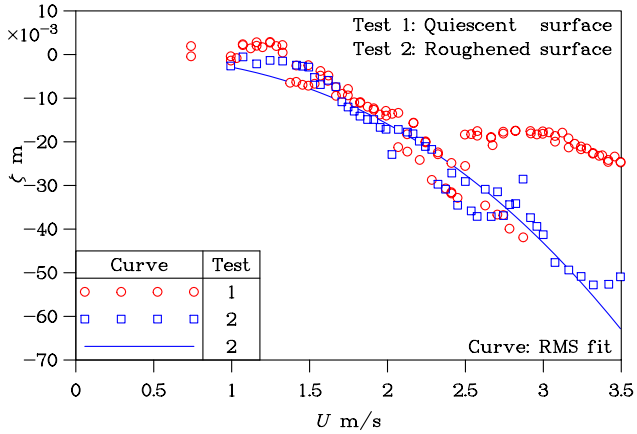

Figure 3: Self Disturbance of Wave Probe

The elevation of the stagnant water in the hollow was then derived from the Bernoulli equation as

$$\zeta^* \quad = \quad C_p U^2/2g\,, \tag{2}$$

where C_p is the (negative) pressure coefficient that would be generated behind the transom stern. The hydrostatic pressure force acting on the surface of the transom stern is estimated on the basis of the *relative elevation* of the calculation point. This contribution to the resistance (positive aft) is:

$$R_{H,1} \quad = \rho g \int_{-T^*}^{\zeta^*} b(x^*, z)(z - \zeta^*)\,\mathrm{d}z\,, \tag{3}$$

in which ρ is the water density and T^* is the dynamic draft at the transom; this is located at the longitudinal coordinate x^*, where the local beam is $b(x^*, z)$.

This method was found to produce excellent agreement between theoretical predictions (based on a pressure coefficient of around -0.25) and the experimental data for the resistance of the vessel.

An extended series of towing-tank experiments on simple rectangular-section ship models was conducted by Doctors (2003). In these tests, the drop in the water level behind the transom was measured for a series of ship models over a range of speeds. These experiments were also supported by the analysis of Robards and Doctors (2003).

More recently, the results of the unwetting of the transom stern of these rectangular-section ship models were applied to a realistic destroyer model tested in a towing tank by Maki, Doctors, Beck, and Troesch (2005). It was demonstrated that reasonable predictions of the unwetting of the transom stern of the destroyer could be achieved in this manner.

1.3 Current Work

In the current work, the experimental data obtained by Doctors (2003) has been expanded upon to include some experimental work on the towing-tank models in which the sinkage and trim were fixed. All the data has been reanalyzed in more detail.

2 Experimental Work

2.1 Transom-Stern Model

Figure 1(a) illustrates the experimental setup employed in the towing-tank experiments. The sinkage s (at the transom) and the trim t of the model were determined via the vertical movements at the two towing posts. In addition to the resistance R_T itself, the free-surface elevation ζ was measured by means of a longitudinally moving electrical-capacitance probe consisting of a pair of thin vertical wires.

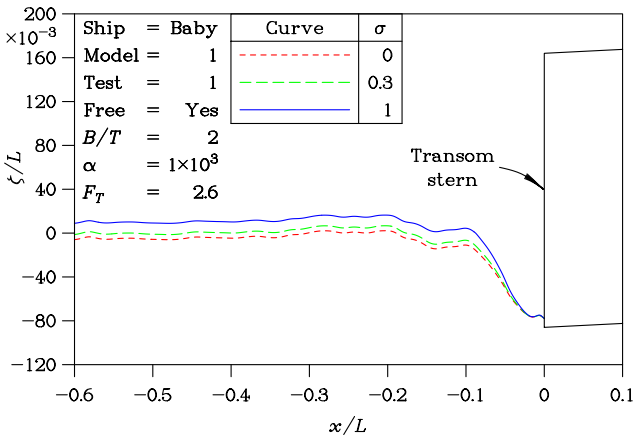

Figure 4: Application of Probe-Wave Correction for Free Trim (a) $F_T = 2.6$

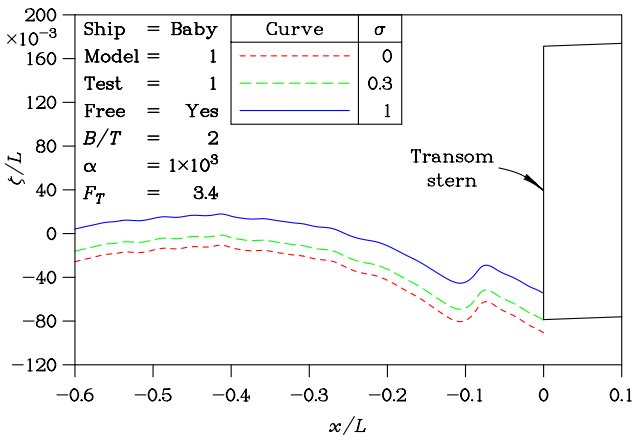

Figure 4: Application of Probe-Wave Correction for Free Trim (b) $F_T = 3.4$

Table 1: Geometric Particulars of Baby Series

Model	Length L (m)	Beam B (m)	Depth D (m)
1	0.8000	0.1000	0.2000
2	0.9514	0.1189	0.2378
3	1.1314	0.1414	0.2828
4	1.3455	0.1682	0.3364
5	1.6000	0.2000	0.4000

Table 2: Coefficients for Baby Series

Particular	Symbol	Value
Maximum-section coefficient	C_M	1.0000
Waterplane-area coefficient	C_{WP}	0.8889
Block coefficient	C_B	0.8889
Prismatic coefficient	C_P	0.8889
Vertical prismatic coefficient	C_{VP}	1.0000

A series of five models, called the Baby series, was towed in the tank. The parent hull is depicted in Figure 1(b). The vessel has vertical sides and a flat bottom. There is a parabolic-waterplane bow section and a parallel aft section. The geometric details are listed in Table 1 and the dimensionless coefficients are given in Table 2.

The loading conditions, 25 in all, are shown in Table 3. The principal linear dimensions of the models were selected so as to increase by the factor $2^{1/4}$. The same factor was employed in choosing the drafts listed in Table 3. As a consequence, a number of the different tests can be considered to be equivalent, except for the relatively small influences of the Reynolds number, the Weber number, and the tank blockage. To gauge the importance of towing-tank blockage, one can consult Table 4, which lists its dimensions. For

Table 3: Test Drafts in Meters for Baby Series

Beam-to-Draft Ratio B/T	Model Number				
	1	2	3	4	5
1.000	0.1000				
1.189	0.0841	0.1000			
1.414	0.0707	0.0841	0.1000		
1.682	0.0595	0.0707	0.0841	0.1000	
2.000	0.0500	0.0595	0.0707	0.0841	0.1000
2.378		0.0500	0.0595	0.0707	0.0841
2.828			0.0500	0.0595	0.0707
3.364				0.0500	0.0595
4.000					0.0500

each loading condition, the model was towed at 25 speeds, corresponding to round values of the (length) Froude number.

2.2 Corrections to Measured Wave Profiles

The wave probe was quite reliable. However, one obvious characteristic of the measurements was the low level of noise in the output signal. This minor problem was dealt with by a numerical wave-smoothing procedure. This is illustrated in the two parts of Figure 2, which correspond to two different transom-draft Froude numbers. The graphs each show two curves. The first curve represents the raw wave-elevation curve. This is indicated by a zero value of the wave-smoothing parameter α. The second curve has been obtained by use of the "graduation" procedure developed by Whittaker (1923) and Henderson (1924). The algorithm has been modified here to permit uneven spacing of the points. It can be

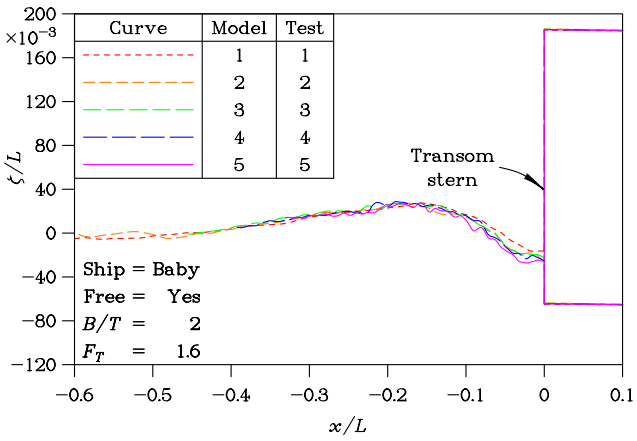

Figure 5: Test of Froude Scaling for Free Trim
(a) $F_T = 1.6$

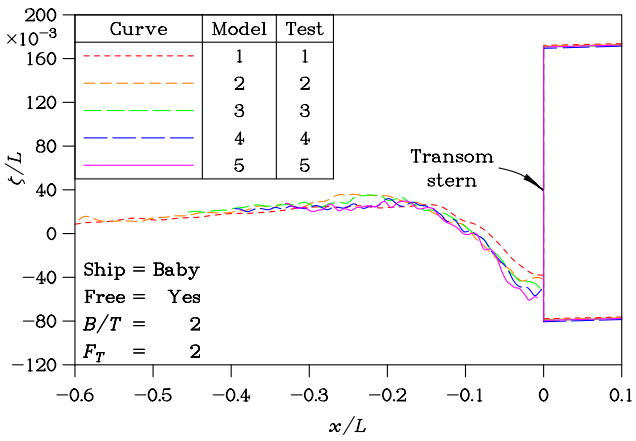

Figure 5: Test of Froude Scaling for Free Trim
(b) $F_T = 2.0$

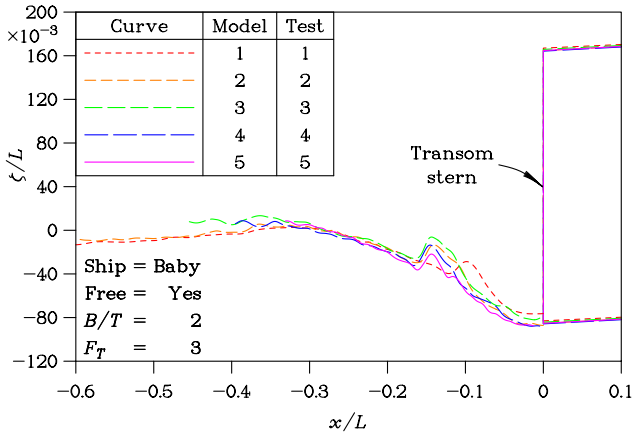

Figure 5: Test of Froude Scaling for Free Trim
(c) $F_T = 3.0$

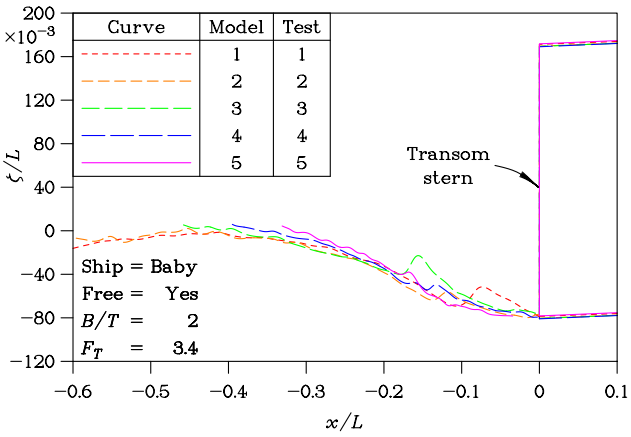

Figure 5: Test of Froude Scaling for Free Trim
(d) $F_T = 3.4$

observed that choosing $\alpha = 1000$ provides a smooth result without losing any of the essential detail.

An additional matter is that the probe also creates its own wave disturbance, which, on the whole, is an effective draw-down of the water surface. This is due to the fact that the after side of the probe wires are ventilated, and increasingly so as the speed increases. Thus, the output readings of wave elevation tend to be too low. This self disturbance is shown in Figure 3. There are two sets of data points. The circles represent the self disturbance when the probe is dragged through calm water. It can be noted that, when the speed U of the probe exceeds about 2 m/s, the trend of the data points becomes bifurcated and there can be two sets of results.

When the water surface was roughened by means of a plastic sheet dragged over the water surface ahead of the probe, the data points indicated with squares was obtained. It is believed that these points are more reliable because, under this condition, almost no bifurcation occurs. Additionally, the roughened surface is more representative of the situation pertaining to the flow behind a transom stern. The least-square fit of this data by a simple power curve is indicated by the continuous curve.

A special numerical algorithm was developed in order to apply this probe wave correction. The wave correction takes account of the fact that there is a zone of relatively dead water behind the transom when it is not fully ventilated; it is assumed that the effective water speed is zero here. The algorithm also assumes that the water speed increases to the proper (inviscid) value for downstream points. Finally, the algorithm also accounts for the fact that the relative water speed should ideally depend on the local wave elevation (via the Bernoulli equation). As a consequence, this wave correction has to be achieved by means of an iteration procedure which is numerically very rapid.

Figure 4 shows the results of applying this wave correction. Despite all the physics incorporated in

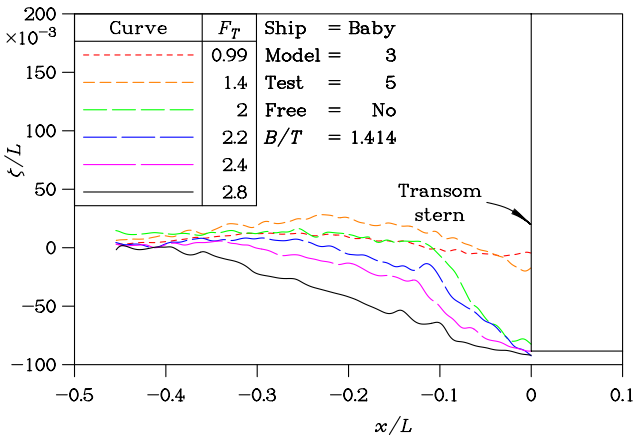

Figure 6: Wave Profiles for Fixed Trim
(a) $B/T = 1.414$

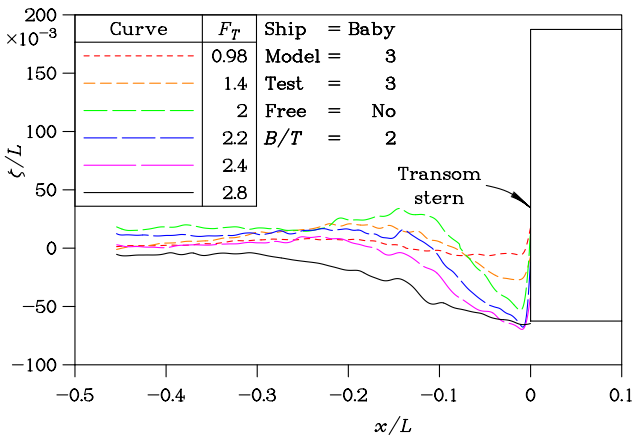

Figure 6: Wave Profiles for Fixed Trim
(b) $B/T = 2.000$

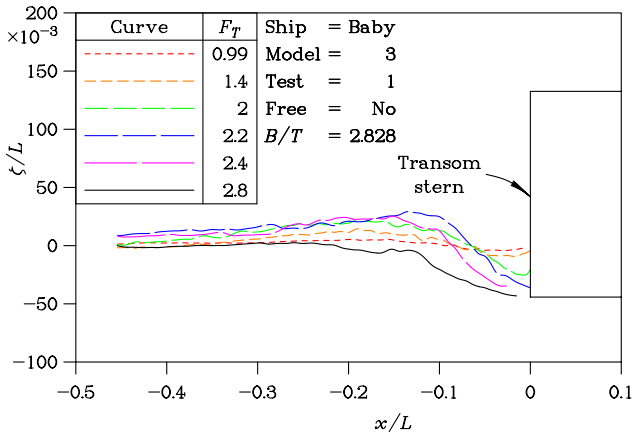

Figure 6: Wave Profiles for Fixed Trim
(c) $B/T = 2.828$

the method, it still overestimates the proper value. We can state this, because we know that the water elevation must match the elevation of the bottom of the transom at high speeds when the transom is fully ventilated. The value of the wave-correction factor σ of 0.30 was chosen to achieve this desired outcome.

2.3 Errors

A study of the scatter of the data in Figure 3 also provides some insight into the matter of measurement errors. Because of the turbulent nature of the flow behind the transom, the error in the measurement of a single point on the free surface is seen to be of the order of ±5 mm. This measurement is the result of a time average of the probe output over a period of about 10 s. The question of unsteadiness is also addressed in Figure 2, where it is seen not to be a critical problem, after the smoothing process is applied.

Table 4: Particulars of Towing Tank

Particular	Symbol	Value
Overall length	l	60.0 m
Width	w	3.550 m
Water depth	d	1.500 m

A major purpose of this paper was to develop algorithms for the hollow length. It is believed that the fitting of analytic curves to the transom wave profile in Figure 11 is a much more significant cause of scatter in the estimate of the hollow length in Figure 12, because of the sensitivity of the mathematics.

3 Wave Profiles

3.1 Effects of Scale in Experiment

A sample of centerplane wave profiles behind the transom stern is plotted in the four parts of Figure 5. The chosen value of the beam-to-draft ratio corresponds to five different loading cases. This permits us to study the effect of scale (the influences of the Reynolds number and the Weber number.) Additionally, there will be some degree of tank blockage.

The plots demonstrate how the water level drops as the speed of the vessel is increased. The fact that the data for the five loading cases does essentially collapse together provides an independent confirmation of the validity of the experiments. Nevertheless, a definite scale effect can be observed. The conclusion is that a model which is too small will lead to a water-level drop which is relatively too small.

One may also note that the wave profiles correctly match the bottom of the transom stern at the higher

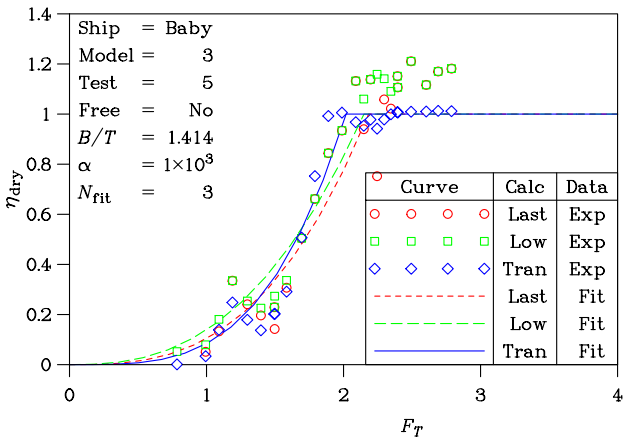

Figure 7: Unwetting of Transom for Fixed Trim (a) $B/T = 1.414$

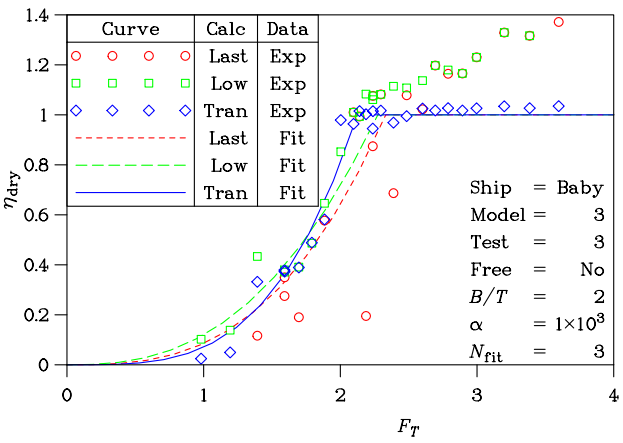

Figure 7: Unwetting of Transom for Fixed Trim (b) $B/T = 2.000$

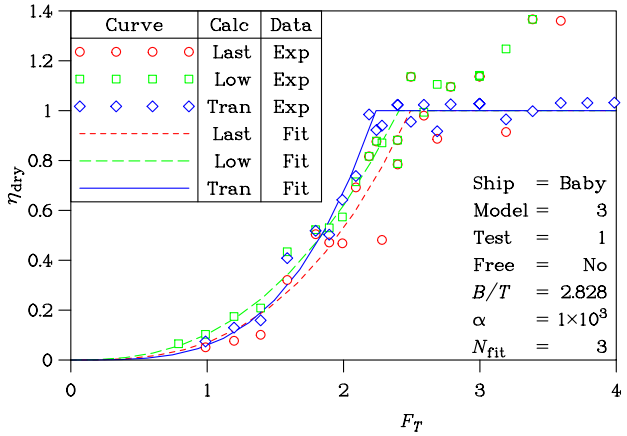

Figure 7: Unwetting of Transom for Fixed Trim (c) $B/T = 2.828$

Froude numbers, following the numerical wave corrections developed in the current phase of the project.

3.2 Effects of Transom-Beam-to-Draft Ratio

Some fixed-trim results are also presented here. These appear in Figure 6 for three different values of the beam-to-draft ratio B/T. The influence of the beam-to-draft ratio is quite small and cannot be detected through a visual inspection of the three parts of this figure. The figures do illustrate, however, how the water level immediately aft of the transom drops as the speed increases. It also shows how the length of the transom-stern hollow increases with speed after full ventilation of the stern takes place.

3.3 Unwetting of Transom

Figure 7 is a plot of the unwetting, or dryness, $\eta_{\rm dry}$ of the transom as a function of the transom-draft Froude number. The unwetting function is defined as:

$$\eta_{\rm dry} \quad = \quad -\zeta^*/T^* \,, \tag{4}$$

in which T^* is the dynamic draft at the transom. (On the other hand, note that the static draft at the transom T is used to form the transom-draft Froude number.)

In each plot, three sets of data are plotted. These are based, respectively, on the last (forwardmost) point in the wave-elevation curve, the lowest point in the wave-elevation curve, and the measurements obtained from a separate wave probe attached directly to the transom itself. It is observed that the best results are obtained from the transom probe, because they indicate that $\eta_{\rm dry}$ approaches unity at high speeds. The other two sets of data (which have not been corrected here for the self-induced wave from the probe) yield points which are too high at the high (fully-ventilated) speeds. Of course, these data points are quite reliable for the partly-ventilated condition, since we are using the forwardmost wave elevation which would then lie in the dead-water region.

By comparison, a regression curve of the form

$$\eta_{\rm dry} \quad = \quad C_1 F_T^{C_2} (B/T)^{C_3} R_{NT}^{C_4} \,, \tag{5}$$

has also been fitted. Here, the transom-draft Reynolds number is defined by $R_{NT} = \sqrt{gT^3}/\nu$, where ν is the kinematic viscosity of the water.

Unwetting functions are also presented for the case of the model being free to sink and trim. The results for three values of the beam-to-draft ratio are shown in Figure 8. Figure 8(b) is particularly instructive, because it clearly shows the influence of model size, that is, the effect of scale. The larger model

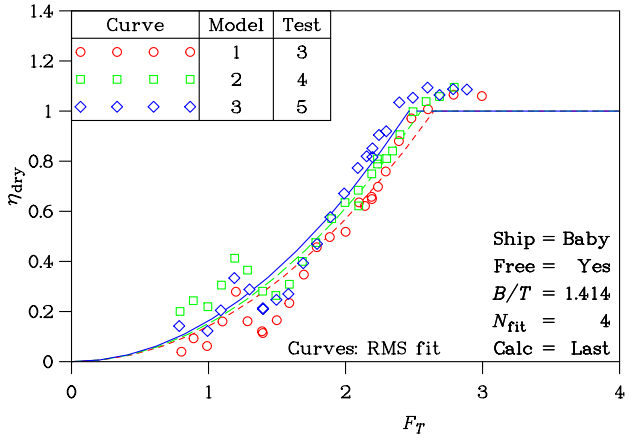

Figure 8: Unwetting of Transom for Free Trim (a) $B/T = 1.414$

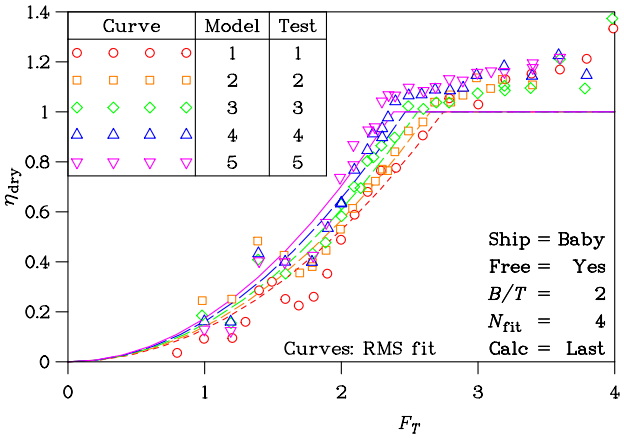

Figure 8: Unwetting of Transom for Free Trim (b) $B/T = 2.000$

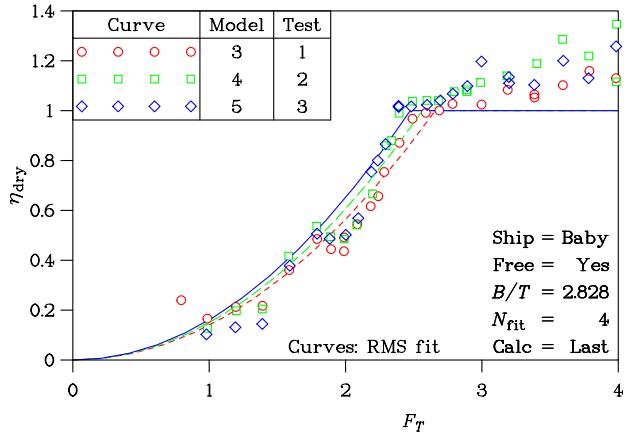

Figure 8: Unwetting of Transom for Free Trim (c) $B/T = 2.828$

number refers to a bigger model, as listed in Table 1. Hence, the unwetting occurs faster for a larger model.

Finally, in Figure 9, we show graphs of the critical transom-draft Froude number F_T^* as a function of the beam-to-draft ratio B/T, with parameter transom-draft Reynolds number R_{NT}. It can be seen that increasing the beam-to-draft ratio has the effect of lowering the critical transom-draft Froude number. There is a similar effect when increasing the transom-draft Reynolds number.

3.4 Sophistication of Fitting Function

The question of the number of factors required to achieve an acceptable regression fit is now considered. The experimental data was fitted using Equation (5) with two, three, and four coefficients.

The root-mean-square error e_{RMS} is plotted as a function of the number of coefficients N_{fit} in Figure 10(a). It is interesting to observe that a good fit is achieved with only two coefficients (that is, just one factor). There is only a relatively small gain in accuracy if the number of factors is increased beyond two. A similar statement can be made about the maximum error $e_{\max}$ — the maximum departure of an experimental point from the fitted regression curve, in Figure 10(b). Finally, the correlation coefficient R^2 is plotted in Figure 10(c).

The coefficients required in the regression equation are presented in Table 5.

3.5 Length of Transom-Stern Hollow

The second major factor describing the transom-stern flow is the length of the hollow created. The precise definition of this hollow is certainly subject to some debate. In order to define the length of the hollow, it was decided to fit a simple parabola to the measured wave profiles.

The parabola is defined, of course, by three coefficients. Two of these coefficients are determined by assuming that the fitted parabola passes through the experimental wave elevation at the transom itself, together with the requirement that the parabola possesses a zero slope there. The curvature is determined by minimizing the root-mean-square error suffered by the fit, in which different lengths of parabolas are considered. This process can be coded by a simple and efficient search process. In order to achieve reliable results, a weighting factor of the inverse fourth root of the hollow length was applied to the error, thereby encouraging the fitted parabola to ignore small waves such as the typical "rooster tail".

Two examples of this analysis are presented in

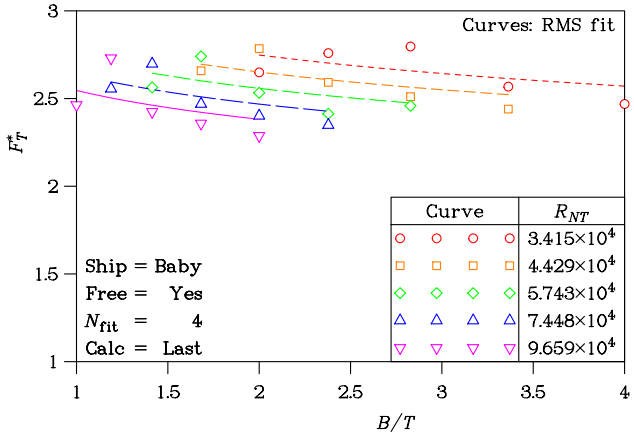

Figure 9: Critical Transom Froude Number for Free Trim (a) Last Point on Wave Profile

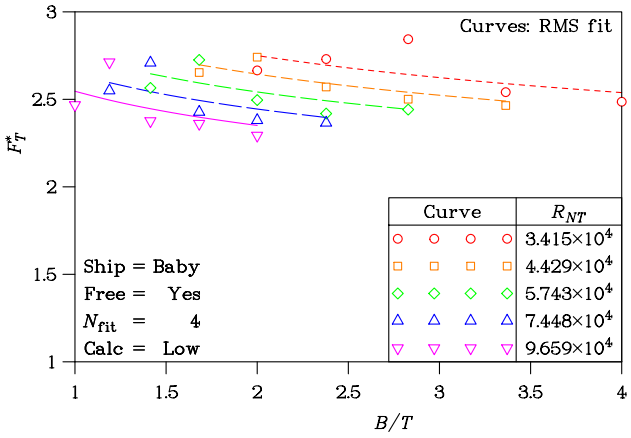

Figure 9: Critical Transom Froude Number for Free Trim (b) Lowest Point on Wave Profile

Table 5: Coefficients of Unwetting Regression Equation

Number of Coefficients N_{fit}	Regression Coefficients			
	C_1	C_2	C_3	C_4
2	0.1578	1.966		
3	0.1577	1.966	0.0002510	
4	0.004879	1.997	0.2302	0.3012

Table 6: Coefficients of Hollow-Length Regression Equation

Number of Coefficients N_{fit}	Regression Coefficients			
	C_1	C_2	C_3	C_4
2	0.06618	3.225		
3	0.05706	3.148	0.2709	
4	0.1956	3.093	0.1948	−0.1015

Figure 11. They pertain to two different transom-draft Froude numbers. It can be noted that the parabola provides an acceptable fit to the shape of the free-surface of the water. Nevertheless, there are some noticeable differences between the outcome of the curve fit for different-size models (the scale effect).

In the current work we are principally concerned with the fully-ventilated case. The dimensionless length L^*/T^* of the transom-stern hollow, obtained in this fashion, is plotted in the three parts of Figure 12, for three different beam-to-draft ratios, respectively. Regression curves for the length, based on a formula corresponding to Equation (5), are also shown. It is assumed, in the partly-ventilated condition, that the *effective hollow length* is essentially constant. This is indicated on the graph. The singularity distribution employed to model the flow is used over this effective ship length. The coefficients required in the regression equation are presented in Table 6.

4 Resistance Calculations

4.1 Components of Resistance

In order to further clarify the phenomenon of the unwetting of the transom stern, we now consider in Figure 13 the components of resistance for some of the tests. These components are the wave resistance R_W, the hydrostatic resistance R_H, and the frictional resistance R_F. The frictional resistance was computed through the 1957 International Towing Tank Committee (ITTC) formula, described by Lewis (1988, Section 3.5).

The data is plotted as a function of the length Froude number F. The components of resistance are rendered dimensionless using the displacement weight W of the vessel. The total resistance is estimated through a simple summation of the components of resistance, as follows:

$$R_T \quad = \quad R_H + f_W R_W + f_F R_F \,. \qquad (6)$$

Here, f_W is the wave-resistance form factor and f_F is the frictional-resistance form factor. For the sake of simplicity, both of these factors were chosen to be unity for the computations presented in Figure 13.

One may note the increasing values of the hydrostatic resistance as the speed increases, until the transom becomes fully-ventilated. The hydrostatic resistance subsequently plateaus or saturates.

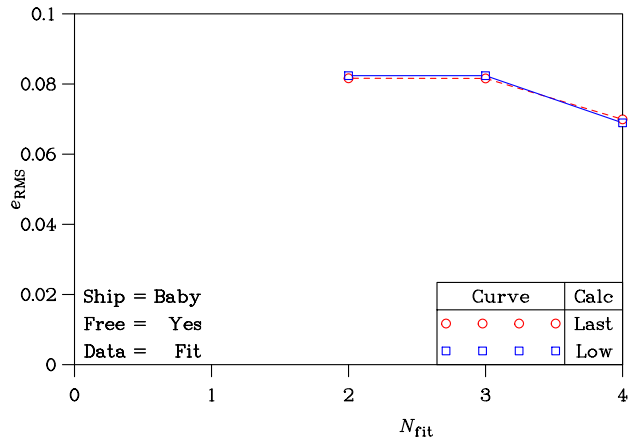

Figure 10: Coefficients in Regression Equation for Free Trim (a) RMS Error

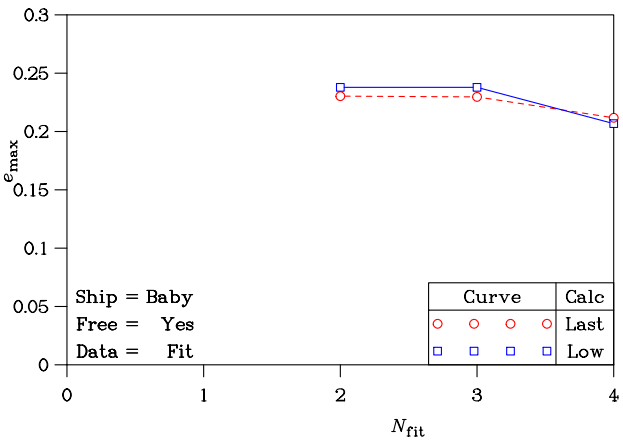

Figure 10: Coefficients in Regression Equation for Free Trim (b) Maximum Error

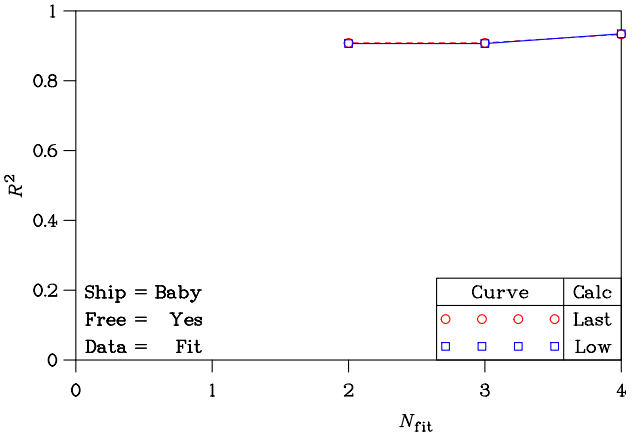

Figure 10: Coefficients in Regression Equation for Free Trim (c) Correlation Coefficient

4.2 Transom-Stern Flow Model

Finally, the total resistance for the Baby models is shown in Figure 14. For the purpose of this exercise, the contribution of the hydrostatic resistance is computed in two ways. In the first (simple) approach, the transom is assumed to be fully-ventilated at all speeds, following the work of Doctors and Day (1997). This is indicated by the symbol "Full". In the second approach, the drop in water level is calculated from the current regression fit to the experimental data according to Equation (5), using the coefficients listed in Table 5. This is indicated by the symbol "Fit".

Regarding the estimation of the transom-stern hollow length, this is achieved in two ways. The first method, indicated by "Hose", is based on the fire-hose concept of Doctors and Day (1997). The second method, indicated by "Fit", is based on the current regression fit, using the coefficients listed in Table 6.

A frictional-resistance form factor $f_F = 1.00$ has been used for all of the theoretical calculations except for the last case, where the value $f_F = 1.18$ has been employed.

One can see that very good agreement for the predictions of the resistance at low values of the Froude number F is achieved using the current idealized model for the drop in water level in the transom-stern hollow region at low speeds, together with the idealized model for the growth of the hollow behind the transom stern. The chosen value of the frictional-resistance form factor (greater than unity) was based on previous work and is seen to provide a small improvement in correlation between the theory and the experiment.

It is particularly encouraging to note the very strong agreement between the computations based on the previous firehose hollow model and the current approach based on actual measurements of the hollow geometry. This provides further confirmation of our understanding of the unwetting process discussed in this paper.

5 Concluding Remarks

5.1 Current Work

The current model for the process of the unwetting of the transom stern has been shown to be in good agreement with the earlier and simpler model utilizing the concept of the bluff-body base suction. It is also encouraging to note that the formula from Oving (1985), namely Equation (1), for the critical transom-draft Froude number, states that its value decreases as the beam-to-draft ratio increases. The current formula for the unwetting process, which is

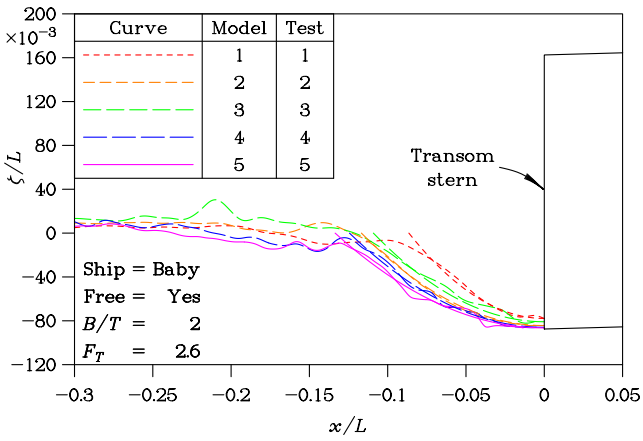

Figure 11: Regression Fit of Transom-Stern Hollow (a) $F_T = 2.6$

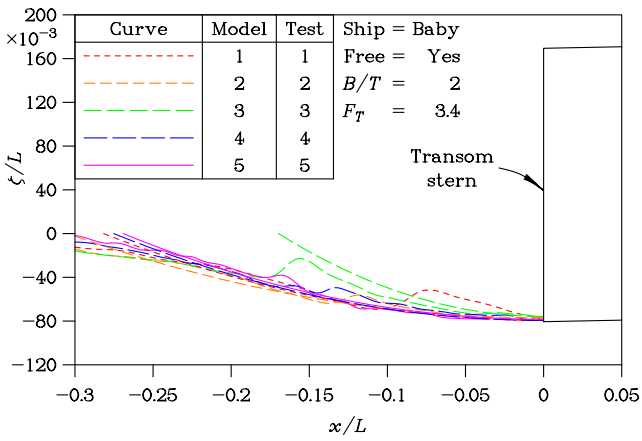

Figure 11: Regression Fit of Transom-Stern Hollow (b) $F_T = 3.4$

Equation (5), with the positive value of the coefficient C_3 from Table 5, suggests the same tendency.

This model for the length of the transom-stern hollow provides the basis of a very good prediction of the total resistance of the vessel when the transom is partly ventilated.

It is pleasing that the results are close to those based on the earlier firehose concept. Thus, we now have a satisfactory resistance-prediction method valid for the entire Froude-number range.

5.2 Future Work

Future work will be directed towards a computational-fluid dynamic (CFD) study of the transom-stern flow. It is hoped, in this way, to estimate numerically the base pressure (negative in value, of course) as a function of the beam-to-draft ratio and the Reynolds number. This will provide a further independent check of our understanding of transom-stern flow, because it should then be possible to correlate the value of the base pressure with the drop in the water level from Equation (2).

6 Acknowledgments

The tests were performed in the Towing Tank at the Australian Maritime College (AMC) by Mr Simon Robards, postgraduate student at UNSW, under the able supervision of Mr Gregor Macfarlane of the AMC.

The authors gratefully acknowledge the assistance of the Australian Research Council (ARC) Discovery-Projects Grant Scheme (via Grant Number DP0209656). This work was also partially supported by Office of Naval Research (ONR) contract N00014-04-1-0266. They are also appreciative to The University of New South Wales for infrastructure support.

References

Couser, P.R., Wellicome, J.F., and Molland, A.F.: "An Improved Method for the Theoretical Prediction of the Wave Resistance of Transom-Stern Hulls Using a Slender Body Approach", *International Shipbuilding Progress*, Vol. 45, No. 444, pp 331–349 (December 1998)

Doctors, L.J.: "Intelligent Regression of Resistance Data for Hydrodynamics in Ship Design", *Proc. Twenty-Second Symposium on Naval Hydrodynamics*, Washington, DC, pp 33–48, Discussion: 49 (August 1998)

Doctors, L.J.: "An Improved Theoretical Model for the Resistance of a Vessel with a Transom Stern", *Proc. Thirteenth Australasian Fluid Mechanics Conference (13 AFMC)*, Monash University, Melbourne, Victoria, Vol. 1, pp 271–274 (December 1998)

Doctors, L.J.: "Effective Prediction of Resistance for High-Speed Hullforms", *Proc. Fourth Japan-Korea Joint Workshop on Ship and Marine Hydrodynamics (JAKOM '99)*, Fukuoka, Japan, pp 305–312 (July 1999)

Doctors, L.J.: "On the Great Trimaran-Catamaran Debate", *Proc. Fifth International Conference on Fast Sea Transportation (FAST '99)*, Seattle, Washington, pp 283–296 (August–September 1999)

Doctors, L.J.: "Hydrodynamics of the Flow be-

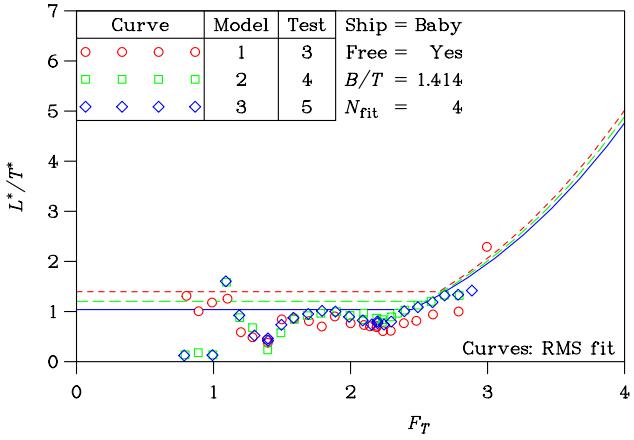

Figure 12: Length of Transom-Stern Hollow
(a) $B/T = 1.414$

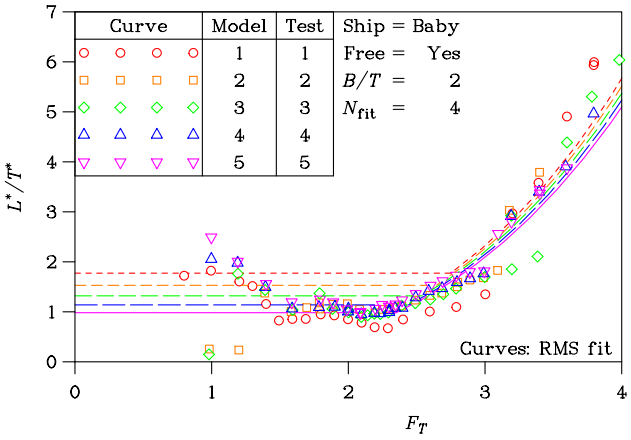

Figure 12: Length of Transom-Stern Hollow
(b) $B/T = 2.000$

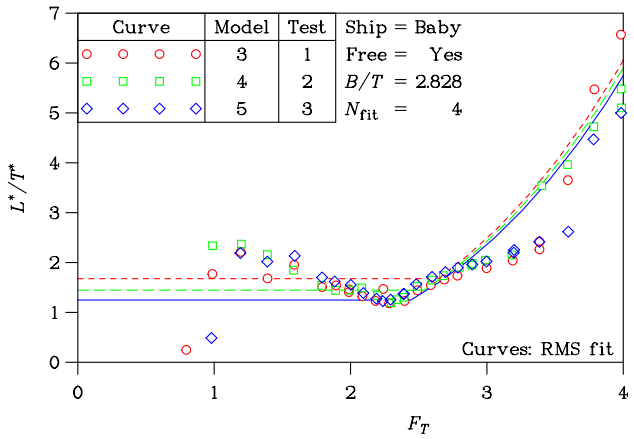

Figure 12: Length of Transom-Stern Hollow
(c) $B/T = 2.828$

hind a Transom Stern", *Proc. Twenty-Ninth Israel Conference on Mechanical Engineering*, Paper 20-1, Technion, Haifa, Israel, 11 pp (May 2003)

Doctors, L.J. and Day, A.H.: "Resistance Prediction for Transom-Stern Vessels", *Proc. Fourth International Conference on Fast Sea Transportation (FAST '97)*, Sydney, Australia, Vol. 2, pp 743–750 (July 1997)

Doctors, L.J. and Day, A.H.: "The Squat of a Vessel with a Transom Stern", *Proc. Fifteenth International Workshop on Water Waves and Floating Bodies (15 IWWWFB)*, Caesarea, Israel, pp 40–43 (February–March 2000)

Doctors, L.J. and Day, A.H.: "Steady-State Hydrodynamics of High-Speed Vessels with a Transom Stern", *Proc. Twenty-Third Symposium on Naval Hydrodynamics*, Val de Reuil, France, pp 12-1–12-14, Discussion: 12-15 (September 2000)

Doctors, L.J. and Day, A.H.: "Nonlinear Effects on the Squat of a Vessel with a Transom Stern", *Proc. Seventeenth International Workshop on Water Waves and Floating Bodies (17 IWWWFB)*, Cambridge, England, pp 33–36 (April 2002)

Doctors, L.J. and Day, A.H.: "Nonlinear Free-Surface Effects on the Resistance and Squat of High-Speed Vessels with a Transom Stern", *Proc. Twenty-Fourth Symposium on Naval Hydrodynamics*, Fukuoka, Japan, Vol. 2, pp 192–205 (July 2002)

Doctors, L.J. and Renilson, M.R.: "Corrections for Finite-Water-Depth Effects on Ship Resistance", *Proc. Eleventh Australasian Fluid Mechanics Conference (11 AFMC)*, University of Tasmania, Hobart, Tasmania, Vol. 1, pp 663–666 (December 1992)

Henderson, R.: "A New Method of Graduation", *Trans. Actuarial Society of America*, Vol. 25, No. 71, pp 29–40 (1924)

Lewis, E.V. (Ed.): *Principles of Naval Architecture: Volume II. Resistance, Propulsion and Vibration*, Society of Naval Architects and Marine Engineers, Jersey City, New Jersey, 327+vi pp (1988)

Lunde, J.K.: "On the Linearized Theory of Wave Resistance for Displacement Ships in Steady and Accelerated Motion", *Trans. Society of Naval Architects and Marine Engineers*, Vol. 59, pp 25–76, Discussion: 76–85 (December 1951)

Maki, K.J., Doctors, L.J., Beck, R.F., and Troesch, A.W.: "Transom-Stern Flow for High-Speed Craft", *Proc. Eighth International Conference on Fast Sea Transportation (FAST '05)*, Saint Petersburg, Russia, 8 pp (June 2005)

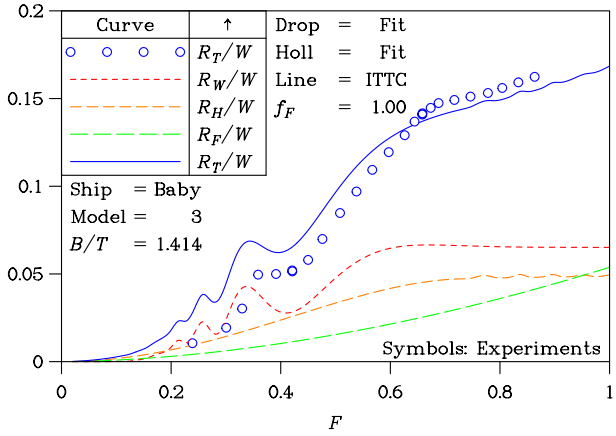

Figure 13: Components of Resistance
(a) $B/T = 1.414$

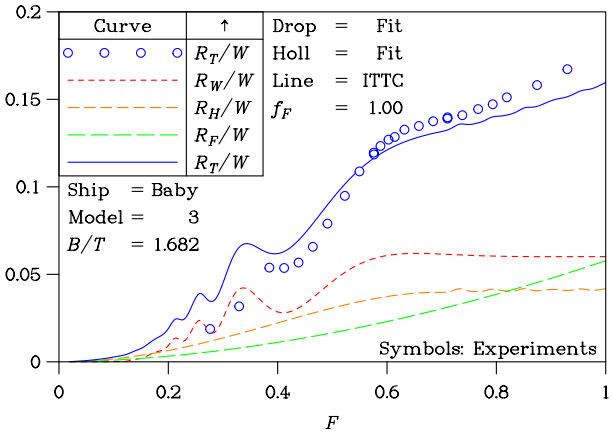

Figure 13: Components of Resistance
(b) $B/T = 1.682$

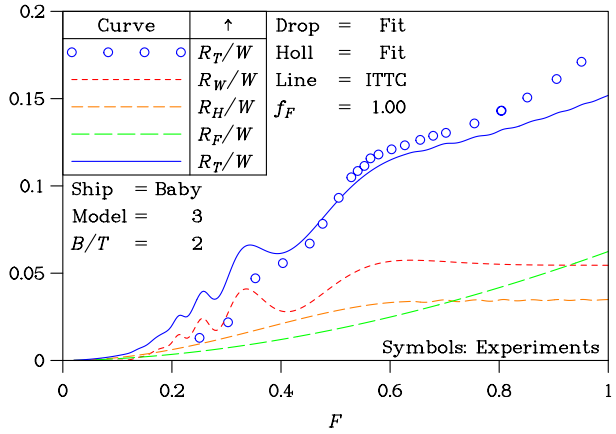

Figure 13: Components of Resistance
(c) $B/T = 2.000$

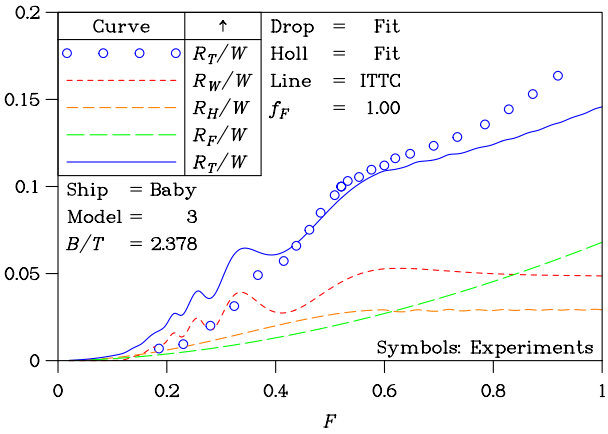

Figure 13: Components of Resistance
(d) $B/T = 2.378$

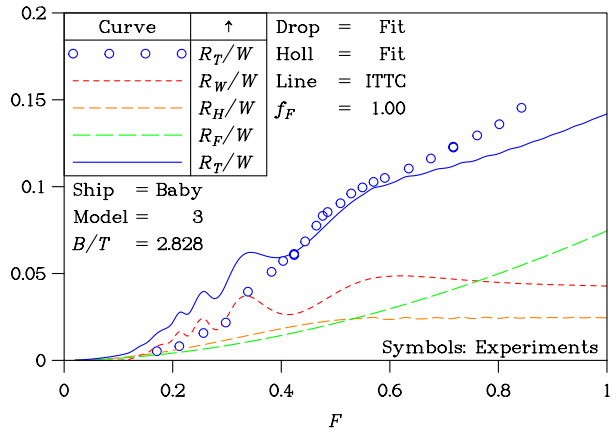

Figure 13: Components of Resistance
(e) $B/T = 2.828$

MICHELL, J.H.: "The Wave Resistance of a Ship", *Philosophical Magazine*, London, Series 5, Vol. 45, pp 106–123 (1898)

MOLLAND, A.F., WELLICOME, J.F., AND COUSER, P.R.: "Theoretical Prediction of the Wave Resistance of Slender Hull Forms in Catamaran Configurations", University of Southampton, Department of Ship Science, Report 72, 24+i pp (March 1994)

OVING, A.J.: "Resistance Prediction Method for Semi-Planing Catamarans with Symmetrical Demihulls", Maritime Research Institute Netherlands (MARIN), Wageningen, 79+i pp (September 1985)

ROBARDS, S. AND DOCTORS, L.J.: "Transom-Hollow Prediction for High-Speed Displacement Vessels", *Proc. Seventh International Conference on Fast Sea Transportation (FAST '03)*, Ischia, Italy, Vol. 1, pp A1.19–A1.26 (October 2003)

SAHOO, P.K. AND DOCTORS, L.J.: "A Study on Wave Resistance of High-Speed Displacement Hull Forms in Restricted Depth", *Proc. Seventh International Conference on Fast Sea Transportation (FAST '03)*, Ischia, Italy, Vol. 1, pp A3.25–A3.32 (October 2003)

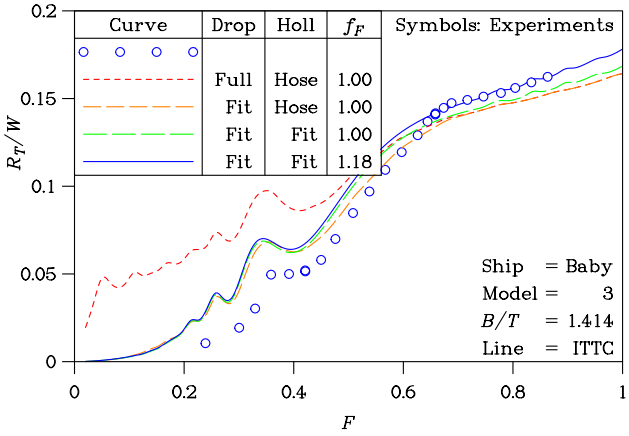

Figure 14: Transom-Stern Flow Model
(a) $B/T = 1.414$

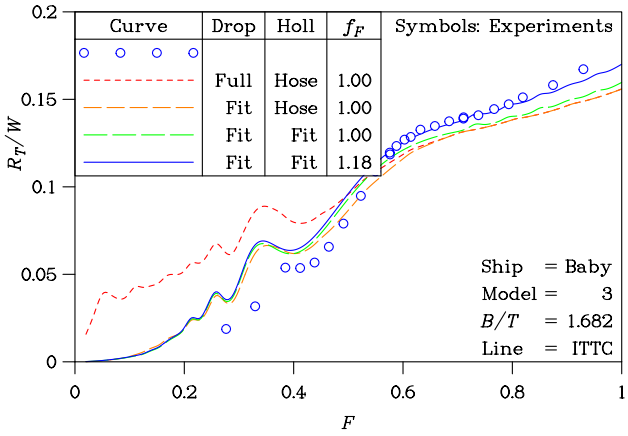

Figure 14: Transom-Stern Flow Model
(b) $B/T = 1.682$

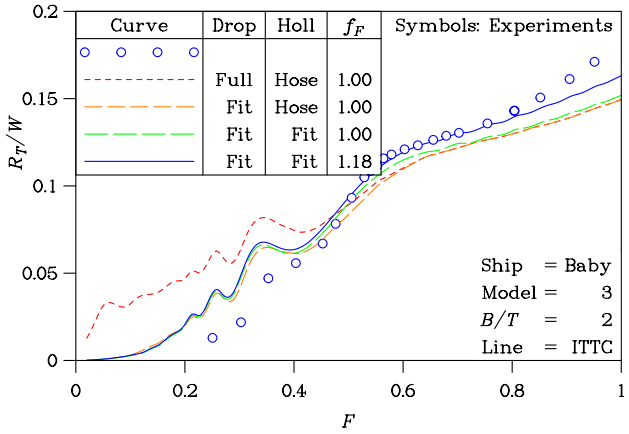

Figure 14: Transom-Stern Flow Model
(c) $B/T = 2.000$

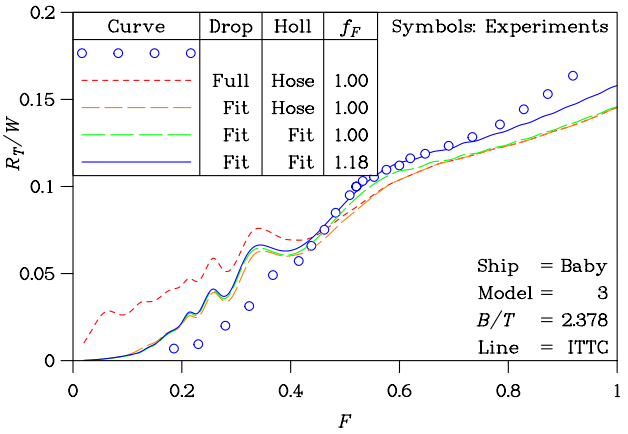

Figure 14: Transom-Stern Flow Model
(d) $B/T = 2.378$

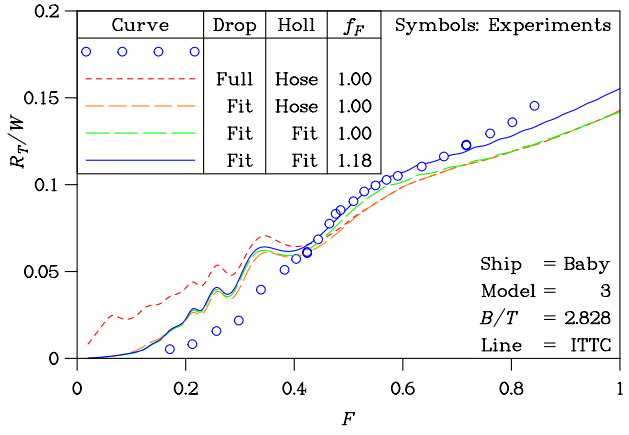

Figure 14: Transom-Stern Flow Model
(e) $B/T = 2.828$

Sahoo, P.K., Doctors, L.J., and Renilson, M.R.: "Theoretical and Experimental Investigation of Resistance of High-Speed Round-Bilge Hull Forms", *Proc. Fifth International Conference on Fast Sea Transportation (FAST '99)*, Seattle, Washington, pp 803–814 (August–September 1999)

Sretensky, L.N.: "On the Wave-Making Resistance of a Ship Moving along in a Canal", *Philosophical Magazine*, Series 7, Supplement, Vol. 22, No. 150, pp 1005–1013 (November 1936)

Toby, A.S.: "The Evolution of Round Bilge Fast Attack Craft Hull Forms", *Naval Engineers J.*, Vol. 99, No. 6, pp 52–62 (November 1987)

Toby, A.S.: "U.S. High Speed Destroyers, 1919–1942: Hull Proportions (to the Edge of the Possible)", *Naval Engineers J.*, Vol. 109, No. 3, pp 155–177, Discussion: 177–179 (May 1997)

Toby, A.S.: "The Edge of the Possible: U.S. High Speed Destroyers, 1919–1942. Part 2: Secondary Hull Form Parameters", *Naval Engineers J.*, Vol. 114, No. 4, pp 55–76 (Fall 2002)

Whittaker, E.T.: "On a New Method of Graduation", *Proc. Edinburgh Mathematical Society*, Vol. 41, pp 63–75 (1923)